

INVESTIGATION OF CAPILLARY FLOW ACROSS A BANK OF ALIGNED FIBERS

Valentin Neacsu¹, Johannes Leisen², Suresh G. Advani¹

¹ *Department of Mechanical Engineering and Center for Composite Materials
University of Delaware, Newark, DE 19716, USA: advani@udel.edu*

² *School of Polymer, Textile and Fiber Engineering
Georgia Institute of Technology, Atlanta, GA 30332, USA: jl167@mail.gatech.edu*

ABSTRACT: This paper introduces two experimental studies of capillary impregnation across fiber tows. The first experimental technique embeds four to five flow detection sensors into a fiber tow at radial locations from the outside to the center of the tow to track the motion of fluid from outside to the center of the tow with time. The second technique based on Magnetic Resonance Imaging (MRI) is a non-intrusive tracking of the flow front as it impregnates the fiber tow. The techniques are compared and contrasted to identify their advantages and limitations. An analytical model that ignores the backpressure of the entrapped air grossly under predicts the saturation time for the tow as compared with the experiments. In order to explain this discrepancy, we include the effect of entrapped air in the analytic model, which slows down the capillary flow. However, other effects such as non-uniform fiber volume fraction within the tow and the ease with which the entrapped air can escape from the tow could also prove crucial as suggested by some of the experimental results.

KEYWORDS: Magnetic Resonance Imaging (MRI), experimental technique, Liquid Composite Molding (LCM), capillary flow, micro-scale flow

INTRODUCTION

In Liquid Composite Molding (LCM) processes, fiber preforms are placed in a mold and then impregnated with resin. The fiber preform consists of fiber tows woven or stitched together. Each fiber tow is made up of thousands of individual fiber strands grouped together in a bundle. The resin has to impregnate not only the empty spaces between the fiber tows but also the gaps between fibers within each fiber tow. The time to completely saturate fiber tows is usually much larger than the time to fill regions in between the fiber tows. Prior analytical work has investigated various aspects of capillary flow of resin through fiber tows. Nevertheless, analytical models are generally based on many simplifications of the tow geometry, as well as assumptions on the material and process parameters, considered constant in time or uniform within the space domain.

This paper is an abridgment of the work we have done, both analytically [1] and experimentally [2, 3]. Preliminary tests we conducted on large replicas of real fiber tows indicated that the analytical models which do not account for the entrapment of air during the capillary impregnation, underestimate the total fill time. Experimental investigations which we are going to detail below show significant discrepancy between the measured times of impregnation and the values calculated from an analytical

solution. These differences seem to be related to the presence of entrapped air and to whether it can dissolve in the resin and escape outward from within the fiber tow. Our first experimental setup inserted electric sensors inside a model tow that was submerged in a resin and recorded the arrival times of the liquid resin at a limited number of radial locations.

The resin arrived at these radial locations much more slowly than predicted by an analytic model so an amendment to the analytical model, to account for the opposing effect of air on the capillary impregnation is proposed to explain the discrepancy. This phenomenological model was subsequently verified using the experimental technique with embedded electric sensors and with a second non-intrusive experimental method, based on Magnetic Resonance Imaging (MRI). Our MRI setup captured the evolution of the 2D flow front interface, with a series of cross-sectional snapshots at selected time intervals.

A comparison between the two experimental techniques is presented, along with their capabilities and limitations. The experimental results show that non-uniformity in fiber volume fraction within the fiber tow and the ability of the air to dissolve in the surrounding liquid does play a significant role in the impregnation dynamics due to the action of capillary forces.

ANALYTICAL MODEL FOR RADIAL IMPREGNATION INTO FIBER TOWS

Our approach built on other analytical models of impregnation within cylindrical fiber tows [4-8]. We also assumed that the capillary impregnation evolved symmetrically only in the radial direction toward the center of the cylindrical fiber tow (Figure 1), and that longitudinal flow as well as body forces can be neglected.

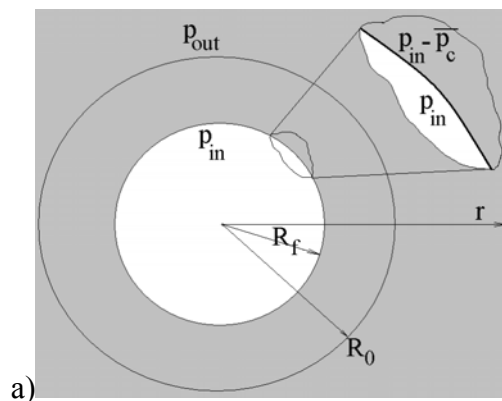


Figure 1. Geometric assumptions of tow impregnation solely by virtue of capillarity

We also derived an equation in finite differences for the more general case, where fiber distribution may vary in radial direction within the porous bundle and liquid parameters may vary in time during the process, as shown below and detailed in [1]:

$$\Delta t = - \frac{\eta(t) \cdot \left[\int_{R_f}^{R_0} \frac{1 - V_f(r)}{r \cdot K(r)} dr \right] \cdot R_f}{p_{out}(t) - p_{in}(R_f) + \overline{p_c}(t, R_f)} \cdot \Delta R_f \quad (1)$$

where t is time, R_f is the flow front radius, Δt and ΔR_f , are finite increments of the time and space coordinates, R_0 is tow's radius, r is the current radial coordinate used for integration, η is liquid's viscosity, V_f is the fiber volume fraction, K is transverse permeability, p_{out} is the pressure of liquid surrounding the tow, p_{in} is the pressure exerted by air opposing the flow, and $\overline{p_c}$ is the average capillary pressure. Some of these parameters can be identified in Figure 1.

If more simplifications are made, such as homogeneity of the porous material (uniform fiber volume fraction) and constant liquid parameters, then a closed form solution can describe the relationship between normalized coordinates time τ and flow front radius ε :

$$\tau = 1 - \varepsilon^2 (1 - 2 \ln \varepsilon) \quad (2)$$

in which $\varepsilon=r/R_0$, r being the location of the resin front and R_0 is the radius of the fiber tow; $\tau=t/t_f^{(0)}$ is the nondimensional time, in which the characteristic time is the analytical fill time $t_f^{(0)}$. The expression for fill time is given in literature for the ideal case where air does not oppose the capillary flow in any way, the driving pressure remaining constant and equal to the capillary pressure. That expression is

$$t_f^{(0)} = \frac{R_0^2 \cdot \eta \cdot (1 - V_f)}{4K \cdot \overline{p_c}} \quad (3)$$

where η is the resin viscosity, V_f is the fiber volume fraction, and K is the transverse tow permeability.

Preliminary experimental investigation

To check how well the above analytical model estimates the tow fill time, we conducted a few preliminary experiments by immersing large replicas of fiber tows (cylindrical samples made of aligned fibers) with five embedded electric sensors along the radial direction in a liquid to let capillarity impregnate the sample spontaneously, without any external application of pressure. The details of the experimental setup is described in the next section (also see Figure 5). Other experimental approaches previously carried out, where we looked for inspiration can be found in [9-12].

The results of these preliminary experiments revealed that the dynamics of the capillary impregnation was different from the analytical closed form solution given by Eqs. (2-3), which under predicted the real fill time as shown in *Figure 2* by a large margin. On the other hand, Eqs. (2-3) seemed to estimate the experimental fill time reasonably well in low-fiber volume fraction tows containing a perforated tube at the center that created an easy path for the entrapped air to escape.

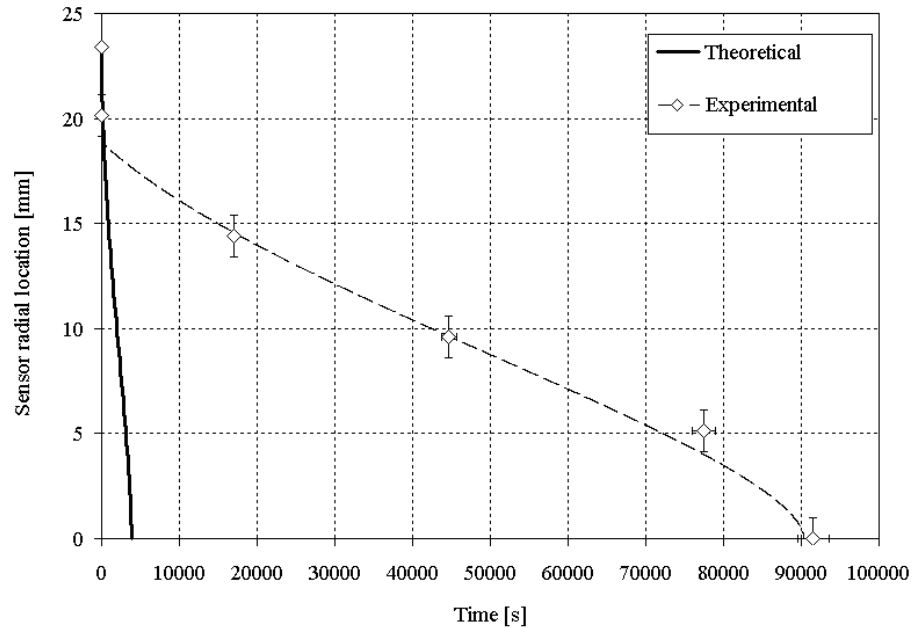


Figure 2. Flow front location vs. time recorded during a preliminary test conducted on a full sample of 70% fiber volume fraction and measuring 47mm in diameter. The dotted curve follows the experimental data points, while the continuous curve represents the analytical estimation, which does not account for the entrapped air effect

These seemed to strongly indicate that air presence and displacement during the capillary impregnation have an opposing effect on the overall dynamics of the process. Although it was observed and measured that during the liquid impregnation air does manage to escape from the sample as emerging bubbles, this was accompanied by a slow-down of the process.

Modification of analytical model

Based on the preliminary experimental findings, we modified the analytical model, to account for the role of air entrapment and displacement. For this purpose, we introduced a correction to account for a gradual loss of air during the inward capillary flow, which has a dual consequence: it lets the air to escape from the porous sample, but at the same time this air displacement slows down the capillary flow front, by exerting a backpressure on it. The proposed model also accounts for the two extreme cases: one, where air escapes outward without exerting any backpressure on the capillary advancement, is equivalent to the situation where air is absent from the tow (e.g. in vacuum assisted processes) and is the only case reflected by the previous simplified analytical model. The other extreme is when the whole quantity of inside air is trapped inside the fiber tow and completely stalls the capillary flow front after a short progression inward.

Without focusing on the exact mechanism of outward air motion, we proposed that there was a pattern for the rate of air loss, uniquely characterized by a scalar parameter δ , which in turn influences the actual fill time of the sample, always greater than the analytical estimation (Figure 3).

In [1], we gave detailed definitions and presented derivations for the rate of air loss and the subsequent fill times, which will not be reproduced here. One important remark is that the model we proposed accounts for both the case where air does not exerts any backpressure and does not slow down the capillary process at all ($\delta=0$) as well as the

other extreme, where air is being trapped inside of the porous sample and completely stops the capillary flow ($\delta=1$) before it reaching the center (Figure 3).

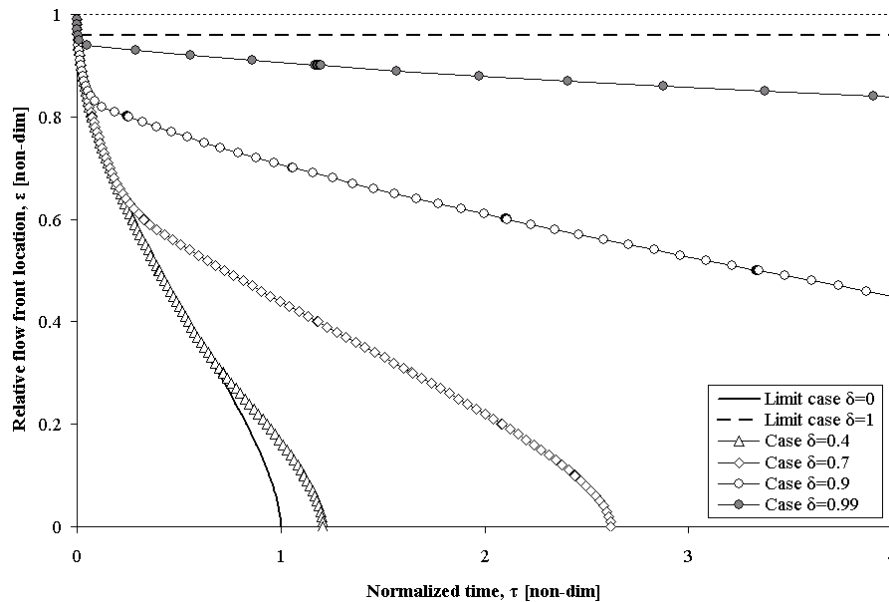


Figure 3. Flow front advancement profile, for several values of parameter δ , in dimensionless coordinates. Case $\delta=0$ (no air effect) is the most favorable case for impregnation, whereas if $\delta=1$ (trapped air), all inside air is compressed until impregnation stops. Any other intermediate value of δ gives a fill time larger than $t_f^{(0)}$

To validate the proposed model and to obtain more insight into what accentuates and what attenuates the opposing role of air displacement on the dynamics of the capillary impregnation, we used two experimental techniques to understand the role of different parameters in the mechanism that slows the impregnation process.

The samples used in both experimental approaches were of two types, as seen in Figure 4. The samples featuring a tube with perforations at the center (Figure 4b) will be referred to as ‘hollow’, being designed to provide the inside air with an easy escape route, without exerting any back-pressure to oppose the capillary flow front advancing inward. The other samples were ‘full’, as shown in Figure 4a. A complete description of the samples is provided in [2] and [3]. The two approaches are described in the next two sections.

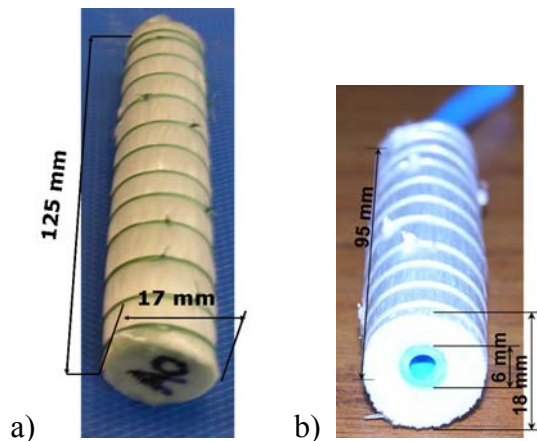


Figure 4. a) ‘Full’ sample of circular cross section; b) ‘Hollow’ sample with perforated inner tube, before ends were sealed

USE OF DISCRETE EMBEDDED ELECTRIC SENSORS

The first experimental setup we used, was based on measuring liquid arrival times at the locations of a few hand-made electric sensors inserted at selected radial locations in the samples (Figure 5a & b). The samples were immersed in a bath of liquid. Due to the electric conductivity of the impregnating liquid, each sensor circuit closed as soon as the liquid reached that location. The data acquisition system attached to the setup read the jump in voltage (Figure 5c) and identified that moment as the arrival time for the corresponding sensor. Because the sensors were perceived as possible sources of perturbations for the capillary liquid, their number was limited to five at the most. The sample diameters were approximately 50 mm, a couple of orders of magnitude thicker than the real fiber tows in composite manufacturing. Full descriptions of samples and tests are given in [2].

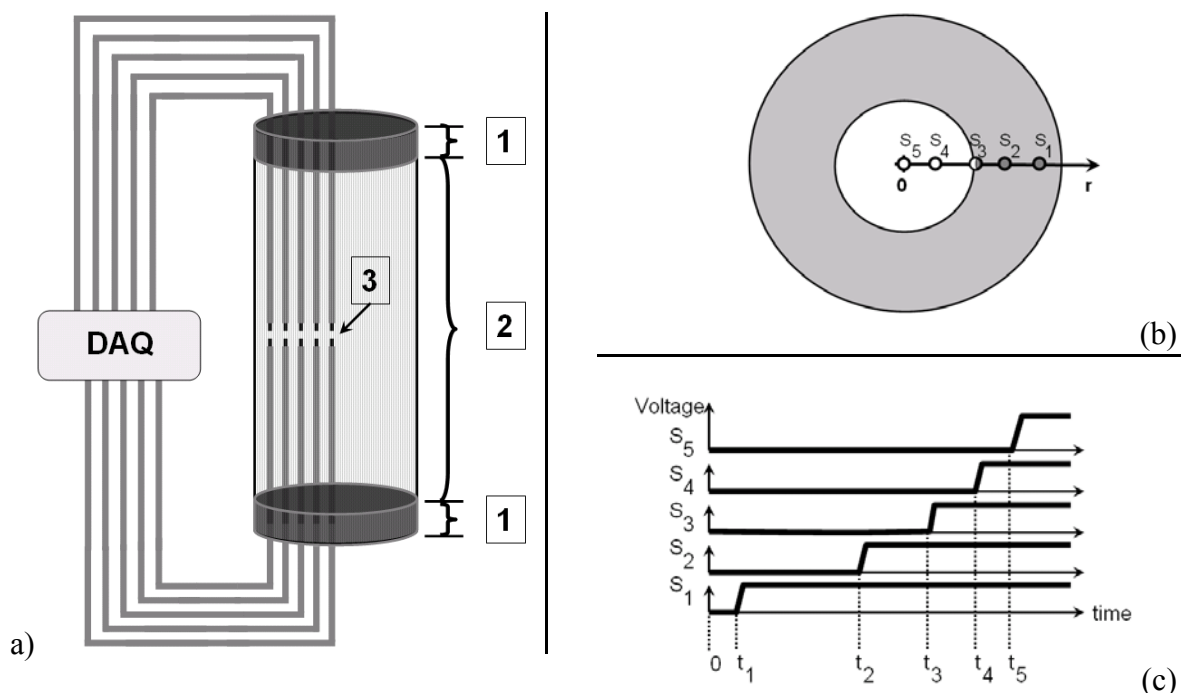


Figure 5 a) Sketch of the setup using electric sensors inserted at radial locations [3]. The cylindrical porous sample [2] and sealed at the ends [1] to minimize longitudinal flow. b) Sensor locations in radial direction S1-S5, shown in cross sectional view. The assumed circular flow front separates the grey (wet) and white (dry) areas. c) Sketch of the electric signals marking the arrival times at sensor locations.

A typical measurement obtained with this technique was presented in *Figure 2* where it is obvious that only few data points were recorded, with relatively significant errors. Among the drawbacks of the technique, its intrusiveness is the most glaring, as sensor wire is much thicker than the individual fibers in the fiber tow sample. Also, the distribution of fibers inside of the samples is perturbed locally by the insertion of the sensors, and this is another cause of concern, as the transverse tow permeability was estimated on the assumption of uniform distribution. In addition to this, not all sensors were identically triggered at the contact of the impregnating liquid, so that in some instances the voltage jumps sketched in *Figure 5b* were not that sudden, consequently making it more difficult to assess the real arrival time of liquid at the location of that particular sensor. At the same time, we found that the technique is not applicable to

smaller samples, because there is not sufficient room to insert more than one sensor at the center.

In spite of these shortcomings, we were able to use the electric sensors to determine that, arrival times at sensors locations in low-fiber-volume-fraction ‘hollow’ samples were comparable to those estimated using Eqs. (2-3). Conversely, for a set of ‘full’ samples made of glass fibers at 45% to 70 % fiber volume fractions, we found that increasing fiber volume fractions V_f are associated with higher values of parameter δ and fill time ratios, which indicate a more inhibiting role of the air escape/dissolution process onto the capillary impregnation. The results presented in Figure 6 show a quadratic trend of fill time ratios vs. V_f , trend well approximated with a R-squared value of 0.98.

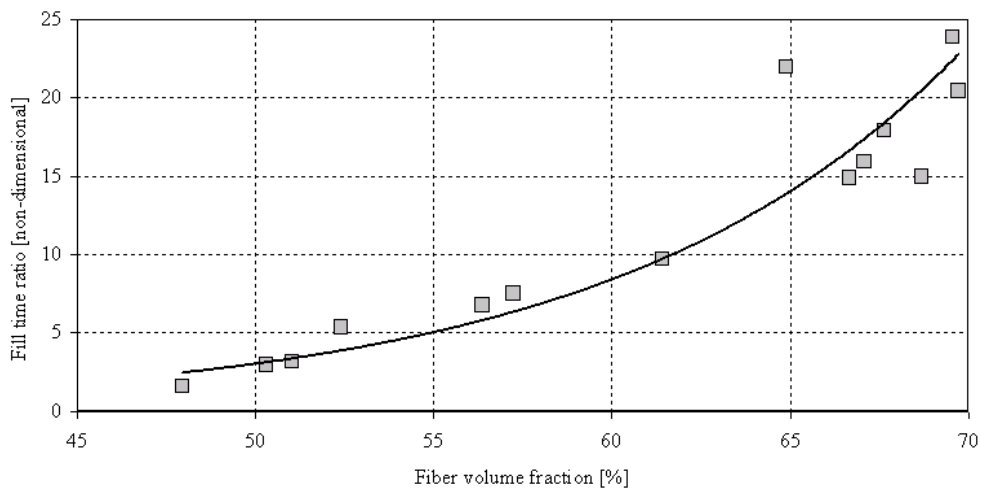


Figure 6. Effect of fiber volume fraction on fill time ratios (calculated by normalizing experimental fill times with respect to the theoretical predictions for the ideal case)

The drawbacks of the technique attracted us to a different approach – Magnetic Resonance Imaging, which is described below.

EXPERIMENTAL APPROACH USING MAGNETIC RESONANCE IMAGING

The primary reason we preferred using Magnetic Resonance Imaging to explore the impregnation dynamics, was due to its ability to yield a two dimensional image of the capillary flow front advancement at a relatively high sampling frequency. Using a Bruker DSX400 MRI spectrometer (by Bruker-Biospin, Rheinstetten/Germany) we were able to record images of the cross-sectional capillary flow front as often as once every 13 seconds. This allowed us to obtain not only a reliable dependence of equivalent flow front radius vs. time, but also to propose a quantification of the irregularity of flow front contour, in connection with the cross-sectional contour of the sample. More technical details on the MRI's applicability to liquid impregnation through porous material have been outlined in [13, 14], while specifics on our experimental study can be found in [3]. A sketch of the experimental setup is shown in *Figure 7a*. The image captured displays dark (dry fibers), grey (wet fibers) and white (surrounding liquid in the test tube) areas, as seen in *Figure 7b*.

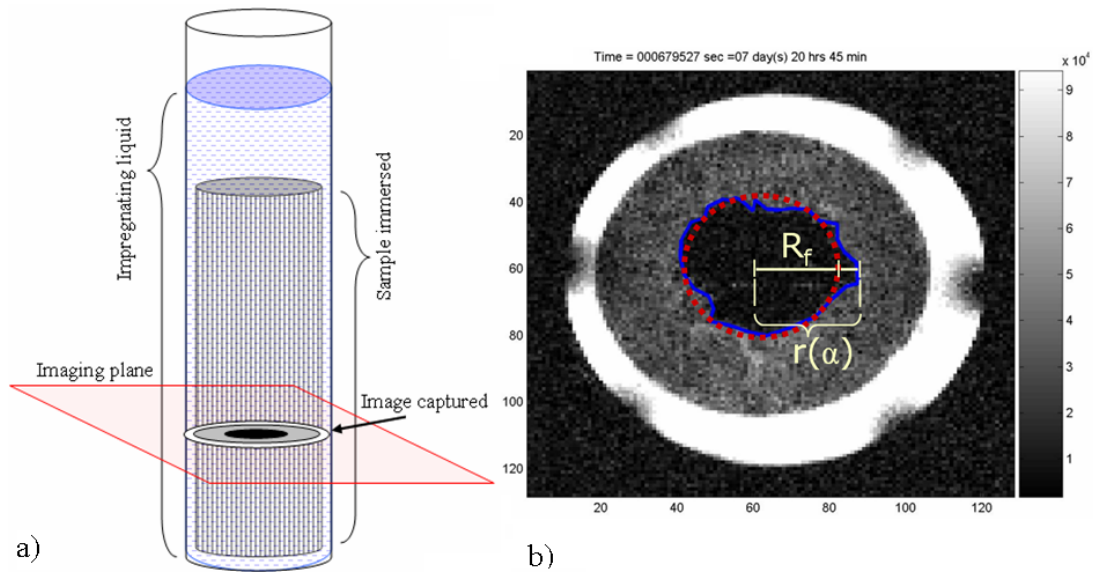


Figure 7. a) Sketch of the MRI setup. b) In addition to the equivalent flow front radius, MRI can also show how much the actual flow front contour (continuous curve) differ from the expected circular pattern (dotted circle).

After data recorded by the spectrometer in digital form are processed, the resulting sequence of frames can serve to generate the flow front advancement vs. time, as seen in Figure 8a. Each data point on the plot corresponds to a frame recorded, but only selected frames are shown in the inserts in Figure 8a, superposed on the experimental curve.

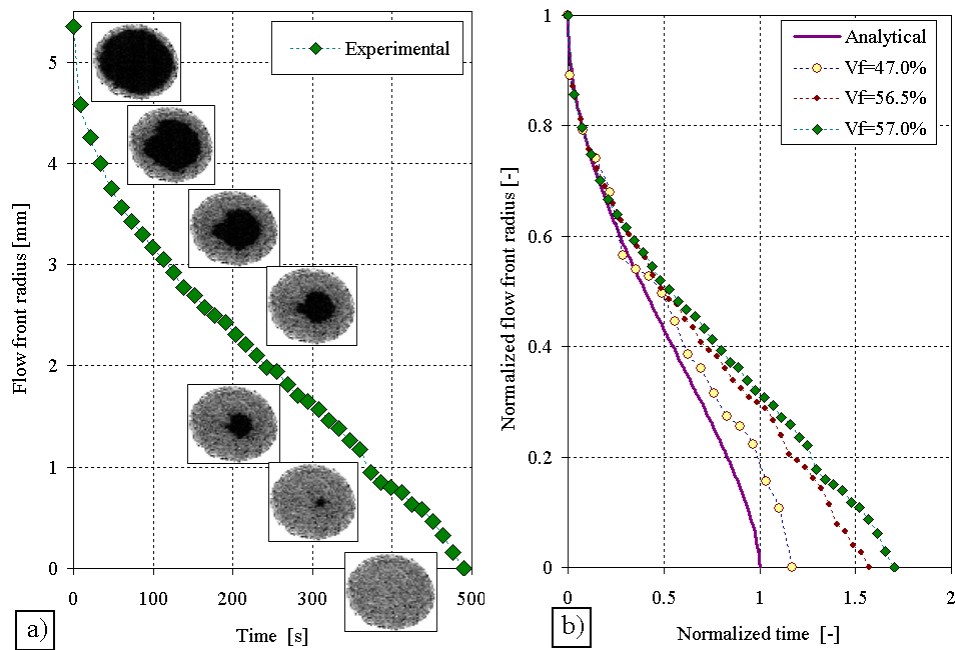


Figure 8a) Typical experimental curve of flow front dependence on time.
 b) Experimental and analytical variation of flow front location $\varepsilon(\tau)$.

We used data recorded experimentally for several samples to generate the profile of capillary impregnation in non-dimensional units, where the flow front location was normalized with respect to the sample radius, and time was normalized with respect to the value of the “ideal fill time” t_f^0 . It is important to specify that the value of this

characteristic time was not derived using Eq. (3), but instead the first few experimental points on plots similar to the one in Figure 8 were used to generate a curve fit of the type expressed by Eq. (2). This approach was based on the assumption that at the beginning of the capillary impregnation, the air does not manifest its opposing effect, and therefore the first stage of the impregnation can be safely approximated with Eq. (2).

This allows us to avoid the challenging aspects of correctly evaluating the transverse tow permeability, as required by Eq. (3). In Figure 8b we have plotted a series of such experimental curves for a set of similar samples of various fiber volume fractions, along with the analytical curve [Eq. (2)], all in non-dimensional coordinates. It is noticeable in Figure 8b that higher the fiber volume fraction, more significant is the role of the air in opposing the flow and slowing it down by exerting back pressure due to the compressed entrapped air.

Another benefit made possible by the high sampling ratio of the MRI data was that we were able to back-calculate the variation of air pressure inside the sample. As seen in Figure 9, a typical profile of the pressure difference ($p_{out} - p_{in} + \bar{p}_c$) normalized with respect to capillary pressure \bar{p}_c , displays an constant trend at the start of the experiment, and then it decreases as the capillary impregnation progresses. This is an interesting aspect, which confirms the fact that air opposition can be neglected at the beginning, but it becomes significant toward the end of the process. Some oscillations of the pressure might confirm the findings of Young [15], who previously showed that the capillary meniscus moves in subsequent jumps across a bank of aligned fibers.

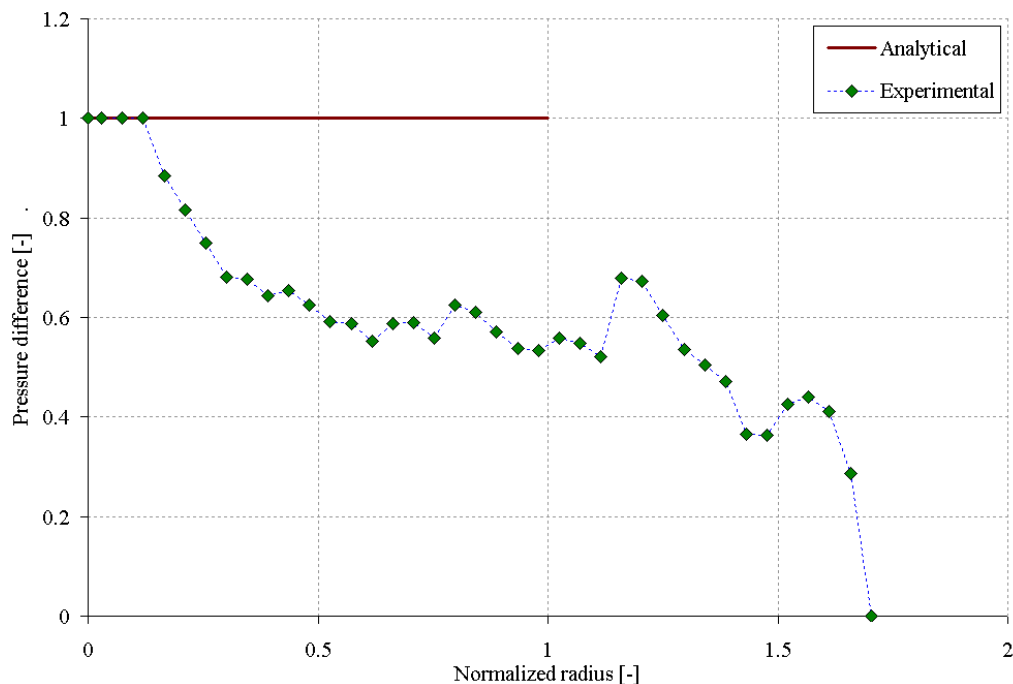


Figure 9. Typical profile of pressure difference driving the capillary flow, as determined indirectly from experimental data (normalized coordinates)

Another interesting finding of our MRI study was that the irregularity of the flow front, which we quantified by means of a parameter, increases during the capillary impregnation due to inherent non-uniformities in fiber distribution within the samples. Moreover with MRI we were able to compare the dynamics of the capillary impregnation as influenced by the nature of the impregnating liquid. The results in

Figure 10 were already normalized by taking into account the viscosities of the liquids, so under ideal conditions one should not expect the viscosity to influence the solution as much as it does. However, we suspect that for the more viscous liquid (corn syrup), maybe the air dissolution or escape is much less probable as compared to water. Thus, the entrapped air is slowed down more significantly in the corn syrup case, where higher back pressure was caused by the compressed air.

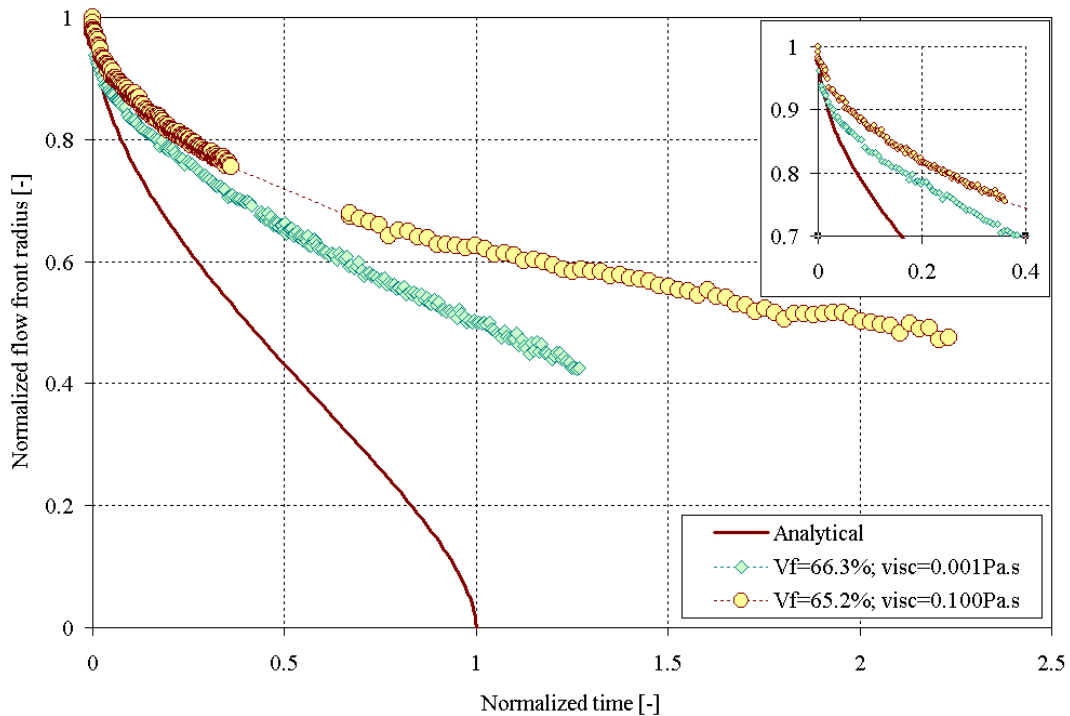


Figure 10. Comparative flow front advancement $\epsilon(\tau)$ plotted against normalized time for two similar samples using corn syrup and water, respectively. The discrepancy suggests that the inhibiting effect of air becomes more prominent for the more viscous liquid.

More details on the results obtainable via MRI in capillary impregnation studies may be found in [3].

Our experimental study revealed that the foremost advantage of the MRI technique is that it can generate detailed data on the shape of the flow front in a non-intrusive way at a very high sampling rate, which could reliably recreate the capillary flow behavior within a porous sample. Thus for us, MRI confirmed our previous finding that higher fiber volume fractions intensify the opposing effect by entrapped air displacement, in addition it revealed the unsymmetric behavior of the capillary flow front.

The limitations of the technique include (i) MRI's inability to accommodate larger samples (the maximum diameter was 23mm, much smaller than the ones tested with electric sensors) or (ii) samples containing metallic elements, (iii) restrictions on the choice of testing liquid (necessarily rich in protons) and (iv) our MRI equipment's inability to test under different pressure levels, other than the atmospheric pressure.

CONCLUSIONS

We have shown that the study of capillary impregnation of fiber tows must account for the role of entrapped air. Our experiments, using two different techniques, one using electric sensors and the other using MRI confirmed that the role of entrapped air becomes more crucial with increasing fiber volume fraction. We compared the two procedures, and found that the former is intrusive and can provide a limited number of data values, while the latter yields detailed information related to visualization of capillary flow and indirect estimation of variation of air pressure inside the fiber tow during the process. MRI was also able to reveal the deviation from radial flow as assumed in the model. The experimental findings definitely shed more light on the fact that higher fiber volume fraction tows of large diameters can be difficult to evacuate completely of air and impregnate with resin.

ACKNOWLEDGMENTS

The authors acknowledge support from the US Office of Naval Research through the AMIPC grant N00014-05-1-0832, and from the US National Textile Center.

REFERENCES

1. V. Neacsu, A. Abu Obaid, and S.G. Advani, "Spontaneous Radial Capillary Impregnation Across a Bank of Aligned Micro-Cylinders - Part I: Theory and Model Development", *International Journal of Multiphase Flow*, vol., 2006, pp.
2. V. Neacsu, A. Abu-Obaid, and S.G. Advani, "Spontaneous Radial Capillary Impregnation Across a Bank of Aligned Micro-Cylinders - Part II: Experimental Investigations", *International Journal of Multiphase Flow*, vol., 2006, pp.
3. V. Neacsu, J. Leisen, and S.G. Advani, "Use of Magnetic Resonance Imaging to Visualize Impregnation across Aligned Cylinders Due to Capillary Forces", *Experiments in Fluids*, vol., submitted 2006, pp.
4. C. Binetruy, B. Hilaire, and J. Pabiot, "The Interactions Between Flows Occurring Inside and Outside Fabric Tows During RTM", *Composites Science and Technology*, vol. 57, 1997, pp. 587.
5. Z. Dimitrovova and S.G. Advani, "Analysis and Characterization of Relative Permeability and Capillary Pressure for Free Surface Flow of a Viscous Fluid across an Array of Aligned Cylindrical Fibers", *Journal of Colloid and Interface Science*, vol. 245, 2002, pp. 325.
6. N. Bernet, V. Michaud, P.-E. Bourban, and J.-A.E. Månson, "An Impregnation Model for the Consolidation of Thermoplastic Composites Made from Commingled Yarns", *Journal of Composite Materials*, vol. 33 (8), 1999, pp. 751.
7. K.J. Ahn, J.C. Seferis, and J.C. Berg, "Simultaneous Measurements of Permeability and Capillary Pressure of Thermosetting Matrices in Woven Fabric Reinforcements", *Polymer Composites*, vol. 12 (3), 1991, pp. 146.

8. K.M. Pillai and S.G. Advani, "Numerical and analytical study to estimate the effect of two length scales upon the permeability of a fibrous porous medium", *Transport in Porous Media*, vol. 21, 1995, pp. 1.
9. G.L. Batch, Y.-T. Chen, and C.W. Macosko, "Capillary Impregnation of Aligned Fibrous Beds: Experiments and Model", *Journal of Reinforced Plastics and Composites*, vol. 15, 1996, pp. 1027.
10. S. Chwastiak, "A Wicking Method for Measuring Wetting Properties of Carbon Yarns", *Journal of Colloid and Interface Science*, vol. 42, 1971, pp. 298.
11. S. Amico and C. Lekakou, "An experimental study of the permeability and capillary pressure in resin-transfer moulding", *Composites Science and Technology*, vol. 61 (13), 2001, pp. 1945.
12. M.E. Foley and J.W. Gillespie, "Modeling the Effect of Fiber Diameter and Fiber Bundle Count on Tow Impregnation During Liquid Molding Processes", *Journal of Composite Materials*, vol. 39 (12), 2005, pp. 1045.
13. J. Leisen and H.W. Beckham, "Quantitative Magnetic Resonance Imaging of Fluid Distribution and Movement in Textiles", *Textile Research Journal*, vol. 71 (12), 2001, pp. 1033.
14. J. Leisen, B. Hojjatie, D.W. Coffin, S.A. Lavrykov, B.V. Ramarao, and H.W. Beckham, "Through-Plane Diffusion of Moisture in Paper Detected by Magnetic Resonance Imaging", *Industrial and Engineering Chemistry Research*, vol. 41, 2002, pp. 6555.
15. W.-B. Young, "Capillary impregnation into cylinder banks", *Journal of Colloid and Interface Science*, vol. 273, 2004, pp. 576.